frontiers in Marine Science

ORIGINAL RESEARCH
published: 24 September 2020
doi: 10.3389/fmars.2020.543124

Aggregate Feeding by the Copepods *Calanus* and *Pseudocalanus* Controls Carbon Flux Attenuation in the Arctic Shelf Sea During the Productive Period

*Helga van der Jagt[1,2], Ingrid Wiedmann[3], Nicole Hildebrandt[1], Barbara Niehoff[1] and Morten H. Iversen[1,2]**

[1] Alfred Wegener Institute Helmholtz Center for Polar and Marine Research, Bremerhaven, Germany, [2] MARUM and University of Bremen, Bremen, Germany, [3] UiT The Arctic University of Norway, Tromsø, Norway

OPEN ACCESS

Edited by:
Cindy Lee,
Stony Brook University, United States

Reviewed by:
Karen Stamieszkin,
College of William & Mary, United States
Slawomir Kwasniewski,
Polish Academy of Sciences, Poland
Jordan Toullec,
UMR 6539 Laboratoire des Sciences de L'Environnement Marin (LEMAR), France

***Correspondence:**
Morten H. Iversen
morten.iversen@awi.de;
morten.iversen@uni-bremen.de

Specialty section:
This article was submitted to Marine Biogeochemistry, a section of the journal Frontiers in Marine Science

Received: 15 March 2020
Accepted: 12 August 2020
Published: 24 September 2020

Citation:
van der Jagt H, Wiedmann I, Hildebrandt N, Niehoff B and Iversen MH (2020) Aggregate Feeding by the Copepods Calanus and Pseudocalanus Controls Carbon Flux Attenuation in the Arctic Shelf Sea During the Productive Period. Front. Mar. Sci. 7:543124. doi: 10.3389/fmars.2020.543124

Up to 95% of the oceanic primary production is recycled within the upper few hundred meters of the water column. Marine snow and zooplankton fecal pellets in the upper water column are often recycled at rates exceeding those measured for microbial degradation, suggesting that zooplankton might be important for flux attenuation of particulate organic carbon in the upper ocean. However, direct evidence for interactions between zooplankton and settling aggregates are still rare. We investigated the importance of zooplankton aggregate feeding for carbon flux attenuation in the upper ocean by determining aggregate ingestion rates and feeding behavior on settling aggregates by the dominant Arctic filter-feeding copepods *Calanus* spp. and *Pseudocalanus* spp. Both genera were observed to detect and feed on settling aggregates. Using *in situ* zooplankton and aggregate abundances in combination with the measured aggregate feeding rates, we calculated that 60–67% of the total carbon flux attenuation at three Arctic locations could be explained by *Calanus* spp. and *Pseudocalanus* spp. aggregate feeding alone. When including microbial degradation of the settling aggregates, we could explain up to 77% of the total carbon flux attenuation. Our results suggest that by directly ingesting and fragmenting settling marine snow, mesozooplankton are key organisms for flux attenuation in Arctic waters.

Keywords: marine snow, zooplankton aggregate feeding, *in situ* optics, sediment traps, zooplankton feeding behavior

INTRODUCTION

The export of particulate organic carbon (POC) from the euphotic zone to the deep ocean is an important process in the global carbon cycle, as it governs the oceanic sequestration of atmospheric carbon dioxide (Siegenthaler and Sarmiento, 1993). This export is driven by the formation and sinking of aggregates, and attenuated by bacterial- and zooplankton-mediated degradation (Buesseler and Boyd, 2009; Iversen et al., 2017). Downward POC flux often follows a power function with increasing depth, showing high flux attenuation in the upper water column

which gets progressively lower in the deeper parts of the water column, resulting in a nearly constant flux in the deep ocean (Martin et al., 1987; DeVries et al., 2012; Marsay et al., 2015; Weber et al., 2016). This low flux attenuation in the deep ocean has been attributed to limited microbial remineralization as a result of low temperature, low dissolved oxygen and high pressure in the deep ocean (Iversen and Ploug, 2013; Tamburini et al., 2013; Marsay et al., 2015). Flux attenuation in the upper few hundred meters of the water column often exceeds the measured microbial remineralization rates, indicating that zooplankton attenuate POC flux in the upper ocean by feeding on the sinking material (Stemmann et al., 2004; Iversen et al., 2010; Jackson and Checkley, 2011).

The importance of zooplankton for flux attenuation has proven difficult to quantify *in situ* (Steinberg et al., 2008; Giering et al., 2014). *In situ* observations and on-board studies have suggested that zooplankton are responsible for decreases in aggregate abundances and changes in particle sizes at the base of the mixed layer (Lampitt et al., 1993; Stemmann et al., 2004; Iversen et al., 2010). Zooplankton feeding activity has also been suggested to be the cause of diel variations in aggregate abundances (Stemmann et al., 2000; Jackson and Checkley, 2011), and *in situ* imaging has shown that thin layers of high aggregate concentrations are also associated with increased zooplankton abundance (Möller et al., 2012).

Observational measurements have suggested that zooplankton aggregate feeding and disaggregation are more important than microbial remineralization for flux attenuation in the upper water column (Iversen et al., 2010). In contrast, respiration measurements and modeling approaches have indicated that zooplankton can be responsible for only 8 to 50% of POC flux attenuation (Steinberg et al., 2008; Giering et al., 2014). As such, Giering et al. (2014) concluded that zooplankton were responsible for only a minor part of the POC flux attenuation via direct aggregate feeding. These authors suggested that fragmentation of settling aggregates enhanced the development of the aggregate-associated microbial communities by providing more time for conversion of detritus into essential biochemical compounds (proteins and lipids) that may be efficiently harvested by the zooplankton, i.e., microbial gardening (Giering et al., 2014; Mayor et al., 2014). These results contrast with observations from experimental studies, in which several copepod species have been observed to directly feed on sinking aggregates and fecal pellets (Koski et al., 2005, 2017; Iversen and Poulsen, 2007; Lombard et al., 2013). These experiments are however difficult to translate to *in situ* POC flux attenuation due to the use of laboratory aggregates formed from fresh phytoplankton material or freshly produced appendicularian houses, while *in situ* aggregates are typically composed of older detritus material and egested compounds with lower organic matter contents (Ploug et al., 2008a).

Specialized flux feeders, such as pteropods and polychaetes, feed on sinking aggregates which they capture below the euphotic zone with their mucous feeding nets (Jackson, 1993). Zooplankton without feeding nets, such as copepods of the genera *Microsetella* (Harpacticoida) and *Oncaea* (Cyclopoida), attach to sinking aggregates and may reside for minutes to hours on the aggregates while feeding on the aggregated material (Alldredge, 1972; Ohtsuka et al., 1993; Koski et al., 2005). The genera *Pseudocalanus* and *Temora* (Calanoida) have also been observed to reside on aggregates both *in situ* and during laboratory experiments, presumably feeding on available organic matter (Möller et al., 2012; Lombard et al., 2013; Koski et al., 2017).

Copepods may recognize the hydrodynamic signals created by settling aggregates (Visser, 2001) or find and follow chemical trails of organic solutes leaking from sinking aggregates (Kiørboe and Thygesen, 2001). Such abilities increase the chance of finding sinking aggregates in the three-dimensional ocean where food sources are patchy, but have so far only been shown in *Temora longicornis* (Lombard et al., 2013). Copepods can fragment fecal pellets and marine snow into smaller, slower-sinking aggregates on which they may feed. This has been observed for *Calanus* and *Pseudocalanus* (Iversen and Poulsen, 2007) as well as other zooplankton (Dilling and Alldredge, 2000; Dilling and Brzezinski, 2004; Goldthwait et al., 2004; Poulsen and Kiørboe, 2005). Fragmentation of sinking aggregates reduces their size-specific sinking velocities and increases their surface to volume ratios, allowing more time for microbial degradation in the upper ocean, thereby increasing POC flux attenuation in the surface ocean (Lampitt et al., 1990; Mayor et al., 2014). Aggregate fragmentation has recently been hypothesized to be the primary process controlling oceanic sequestration of settling carbon (Briggs et al., 2020).

Direct evidence for interactions between zooplankton and settling aggregates are still rare and therefore their role for flux attenuation in the ocean is unclear. This is especially true for polar environments where ice-conditions make access difficult. In this study we investigated the quantitative importance of the dominant mesozooplankton genera, i.e., the calanoid copepods *Calanus* and *Pseudocalanus* as well as balanid nauplii, for POC flux attenuation in three Arctic regions. The Arctic has high POC export out of the surface ocean but this export is strongly attenuated in the upper water column (Wassmann et al., 2003). We incubated freshly collected copepods and balanid nauplii with *in situ* collected aggregates to determine aggregate grazing rates, and used direct video observations to investigate copepod and balanid nauplii feeding behavior. We combined these measurements with vertical profiles of *in situ* zooplankton and aggregate abundances and species- and size-distributions to calculate the impact of zooplankton aggregate feeding on flux attenuation in the upper 50 m of the water column. The POC flux attenuation was directly measured from sediment trap deployments and derived from *in situ* profiles of aggregate abundance and size-distribution using an *in situ* camera system.

MATERIALS AND METHODS

Sampling and incubation experiments were performed on-board the *R/V Helmer Hanssen* during the ARCEx cruise from 17 to 29 May 2016 in Hornsund, Erik Eriksen Strait, and Storfjorden (**Figure 1** and **Table 1**).

FIGURE 1 | Overview of the research locations Hornsund, Storfjorden and Erik Eriksen Strait during the Helmer Hanssen ArcEx cruise around Svalbard.

TABLE 1 | Overview of the deployments of the marine snow catcher (MSC), WP-2-net, sediment trap, *in situ* camera (ISC), and MultiNet (MN).

Location	Device	Date	Depth	Notes
Hornsund	MSC	19.05.2016	20 m	*Pseudocalanus* experiments
	WP-2	19.05.2016	90 m	*Pseudocalanus* experiments
	WP-2	19.05.2016	113 m	
	Trap	19.05.2016	20, 30, 40, 60, 90 m	Anchored
	ISC	19.05.2016	122 m	
	ISC	20.05.2016	95 m	
	ISC	20.05.2016	93 m	
	ISC	20.05.2016	126 m	
	ISC	20.05.2016	112 m	
	ISC	20.05.2016	135 m	
Erik Eriksen St.	MSC	23.05.2016	22 m	*Calanus* experiments
	WP-2	23.05.2016	40 m	*Calanus* experiments
	Trap	23.05.2016	30, 40, 60, 90, 120, 150 m	Attached to ice floe
	MN	23.05.2016	25, 50, 100, 150, 250 m	
	ISC	23.05.2016	263 m	
	ISC	23.05.2016	262 m	
	ISC	23.05.2016	235 m	
	ISC	23.05.2016	251 m	
	ISC	23.05.2016	61 m	
Storfjorden	MSC	21.05.2016	25 m	Balanid nauplii experiments
	WP-2	21.05.2016	95 m	Balanid nauplii experiments
	WP-2	21.05.2016	95 m	
	ISC	21.05.2016	86 m	

Zooplankton Collection

We collected the most abundant zooplankton genera at each station for incubations and video recordings using a WP-2 net with a mesh size of 200 μm and equipped with a large, filtering cod-end to minimize damage to the zooplankton (**Table 2**). *Pseudocalanus*, *Calanus*, and balanid nauplii were collected in Hornsund, Erik Eriksen Strait, and Storfjorden, respectively. The content of the cod-end was directly transferred into several large containers filled with surface water and stored at *in situ* temperature (0°C) in darkness. Individual adult and copepodite stage copepods and balanid nauplii were sorted using a stereo microscope and a wide-bore pipette. Sorted zooplankton were incubated overnight in GF/F filtered seawater in 25 L food grade buckets to allow them to empty their guts. The next morning, we selected healthy and actively swimming copepods and balanid nauplii and transferred them to either roller tanks, to determine grazing on aggregates, or an aquarium to record aggregate feeding behavior. As the zooplankton organisms needed to be handled quickly, we did not identify *Calanus* species or developmental stages prior to incubation but picked specimens of similar sizes (prosome length: 2.9 ± 0.5 mm) for the experiments. After the incubations, the experimental individuals were preserved in 4% formaldehyde solution in seawater, and the species were identified after the cruise in the laboratory. Identification of species of the genus *Calanus* (*C. hyperboreus, C. glacialis*, and *C. finmarchicus*) was made on the basis of prosome length measurements for each developmental stage according to Arnkværn et al. (2005). The identification showed that the *Calanus* specimens in the incubations were a mixture of C5 stages of *C. hyperboreus* and C4, C5, and adult stages of *C. glacialis*. We therefore refer to these collectively as *Calanus* spp. hereafter (**Table 3**).

Collection of Aggregates

Intact aggregates were collected with a Marine Snow Catcher (MSC, Ocean Scientific International Ltd., United Kingdom) at each station where the zooplankton were collected. The MSC is a 100 L water sampler which does not destroy large aggregates during sampling (e.g., Belcher et al., 2016a; Busch et al., 2017; Flintrop et al., 2018). The MSC was lowered open to 10 m below the fluorescence maximum whereupon it was closed immediately using a releaser and a messenger before it was brought back on deck. We left the MSC on deck for approximately 3 h to allow the aggregates to settle to the bottom compartment. The height of the MSC was 2 m, which means that aggregates sinking faster than 18 m d^{-1} would able to sink from the top to the bottom of the MSC during 3 h. Hereafter, we gently drained and GF/F filtered the overlaying water and stored it for use during grazing incubations, video observations, and acclimation of the copepods. The bottom part of the MSC was brought to the

TABLE 2 | Zooplankton abundance in the upper 25 m of the water column at Hornsund, Erik Eriksen Strait, and Storfjorden.

Zooplankton type	Copepod stage	Hornsund – WP-2		Erik Eriksen Strait – MN		Storfjorden – WP-2	
		Abundance (ind m^{-3})	Biomass (mg DW)	Abundance (ind m^{-3})	Biomass (mg DW)	Abundance (ind m^{-3})	Biomass (mg DW)
C. finmarchicus	C1	0.00	0.00	0.00	0.00	0.00	0.00
C. finmarchicus	C2	0.00	0.00	0.00	0.00	6.65	0.31
C. finmarchicus	C3	3.32	0.15	0.00	0.00	9.97	0.46
C. finmarchicus	C4	6.65	0.85	37.33	4.78	3.32	0.43
C. finmarchicus	C5	8.31	2.28	93.33	25.57	46.55	12.75
C. finmarchicus	Adult female	4.99	1.63	10.67	3.49	40.00	13.05
C. finmarchicus	**Sum of all stages**	**23.27**	**4.91**	**141.33**	**33.84**	**106.39**	**26.99**
C. glacialis	C1	3.32	0.02	10.67	0.07	16.62	0.12
C. glacialis	C2	1.66	0.07	0.00	0.00	3.32	0.14
C. glacialis	C3	6.65	0.29	2.67	0.12	0.00	0.00
C. glacialis	C4	38.23	6.46	162.67	27.49	19.95	3.37
C. glacialis	C5	11.64	9.05	32	24.90	13.30	10.35
C. glacialis	Adult female	18.29	16.27	42.67	37.93	33.25	29.59
C. glacialis	**Sum of all stages**	**79.79**	**32.17**	**250.67**	**90.55**	**86.44**	**43.57**
C. hyperboreus	C1	14.96	0.11	53.33	0.37	83.12	0.58
C. hyperboreus	C2	0.00	0.00	0.00	0.00	6.65	0.29
C. hyperboreus	C3	0.00	0.00	0.00	0.00	0.00	0.00
C. hyperboreus	C4	0.00	0.00	0.00	0.00	0.00	0.00
C. hyperboreus	C5	1.66	1.70	53.33	54.45	6.65	6.79
C. hyperboreus	Adult female	0.00	0.00	0.00	0.00	0.00	0.00
C. hyperboreus	**Sum of all stages**	**16.62**	**1.80**	**106.67**	**54.83**	**96.42**	**7.66**
Pseudocalanus spp.	C1	0.00	0.00	0.00	0.00	0.00	0.00
Pseudocalanus spp.	C2	0.00	0.00	0.00	0.00	0.00	0.00
Pseudocalanus spp.	C3	1.66	0.04	0.00	0.00	0.00	0.00
Pseudocalanus spp.	C4	34.91	0.80	5.33	0.12	9.97	0.23
Pseudocalanus spp.	C5	118.03	2.72	5.33	0.12	49.87	1.15
Pseudocalanus spp.	Adult female	29.92	0.69	16.00	0.37	123.01	2.83
***Pseudocalanus* spp.**	**Sum of all stages**	**184.52**	**4.24**	**26.67**	**0.61**	**182.86**	**4.21**
Other copepods		92.68	2.45	186.67	4.93	132.99	3.51
Calanoid nauplii		8.83	0.01	3469.33	3.47	4511.58	4.51
Balanid nauplii		**160.72**	**0.32**	**0.00**	**0.00**	**2686.34**	**5.37**
Other zooplankton		4.05	0.15	10.67	0.40	43.22	1.61
Investigated zooplankton							
Calanus spp.	**Sum of all**	119.68	38.88	**498.67**	179.22	289.25	78.22
Pseudocalanus spp.	**Sum of all**	**184.52**	4.24	26.67	0.61	182.86	4.21
Balanid nauplii		160.72	0.32	0.00	0.00	**2686.34**	5.37

At Hornsund and at Storfjorden the zooplankton were collected by a WP-2 net with mesh-size of 200 μm. At Erik Eriksen Strait the zooplankton were collected by a MultiNet with a mesh-size of 200 μm. Bold fonts in the upper panel indicate the sum of all stages for Calanus finmarchicus, C. glacialis, C. hyperboreus, Pseudocalanus spp. and balanid nauplii. Bold fonts in the lower panel indicate the most abundant of the investigated zooplankton at each of the three regions.

laboratory and kept at 0°C in darkness until the aggregates were picked for experiments.

Grazing Incubations

Grazing rates on settling aggregates of balanid nauplii, adults and copepodites IV and V of *Calanus* spp., and egg-bearing females of *Pseudocalanus* spp. were determined in roller tanks (1.15 L, diameter: 14 cm, depth: 7.5 cm). Roller tanks are cylindrical aquariums that are rotated with three rounds per minute on a roller table. The rotation creates solid body rotation of the water within the roller tanks, which gently keeps aggregates and zooplankton suspended without introducing turbulence, much like settling through an infinite tube (see Shanks and Edmondson, 1989). We executed one incubation experiment for each of the three zooplankton organisms. For each experiment, five roller tanks were filled with GF/F filtered water from the MSC and 20 balanid nauplii, three or four *Calanus*, or ten *Pseudocalanus* females gently added to each roller tank (**Table 3**). We picked similar types, sizes and amounts of aggregates from the MSC collection into 10 Petri dishes for each experiment. We removed all copepod fecal pellets from the Petri dishes and photographed each dish to analyze the aggregate sizes in order to determine

TABLE 3 | Overview of the three grazing incubations; *Calanus* spp. experiment, *Pseudocalanus* spp. experiment, and balanid nauplii experiment.

Experiment/roller tank	Incubation time (days)	Zooplankton incubation species (stage)	Start POC_{AGG} (μg POC)	End POC_{AGG} (μg POC)	Ingestion rate (μgPOC ind^{-1} d^{-1})
Calanus* spp. *experiment					
Roller tank 1	1.15	*C. glacialis* (2xC4, 2xC5)	80	32.9	10.22
Roller tank 2	1.24	*C. glacialis* (1xm, 1xf, 1xC4)	109.5	37.0	19.47
Roller tank 3	1.26	*C. hyperboreus* (4xC5)	85.2	35.8	9.81
Roller tank 4	1.29	*C. hyperboreus* (2xC5) *C. glacialis* (2xC4)	100.7	15.6	16.48
Roller tank 5	1.33	*C. hyperboreus* (2xC5) *C. glacialis* (1xC4, 1xC5)	107.6	48.5	11.11
Average ± SD	1.25 ± 0.07		96.60 ± 13.32	33.96 ± 11.86	13.43 ± 4.33
Pseudocalanus* spp. *experiment					
Roller tank 1	1.54	10 x *Pseudocalanus* spp.	98.3	27.4	4.60
Roller tank 2	1.54	10 x *Pseudocalanus* spp.	129.2	43	5.60
Roller tank 3	1.63	10 x *Pseudocalanus* spp.	87.4	38.9	2.98
Roller tank 4	1.65	10 x *Pseudocalanus* spp.	164.1	43.5	7.31
Roller tank 5	1.69	10 x *Pseudocalanus* spp.	160.2	17.2	8.46
Average ± SD	1.61 ± 0.07		127.80 ± 34.90	34.00 ± 11.41	5.79 ± 2.17
Balanid nauplii experiment	**Incubation time (days)**	**Zooplankton incubation (ind roller $tank^{-1}$)**	**FP production (# ind^{-1} d^{-1})**	**FP production (μgPOC ind^{-1} d^{-1})**	**Ingestion rate (μgPOC ind^{-1} d^{-1})**
Roller tank 1	1.69	20 x balanid nauplii	1.54	0.05	0.14
Roller tank 2	1.79	20 x balanid nauplii	1.68	0.05	0.15
Roller tank 3	1.85	20 x balanid nauplii	1.81	0.06	0.16
Roller tank 4	2.35	20 x balanid nauplii	1.23	0.04	0.11
Roller tank 5	2.43	20 x balanid nauplii	1.24	0.04	0.11
Average ± SD	2.02 ± 0.34		1.5 ± 0.26	0.05 ± 0.01	0.13 ± 0.02

The table shows the incubation time and number, type, and stage of zooplankton incubated for each roller tank in each experiment. For the Calanus and Pseudocalanus experiments we were able to measure start and end concentrations of aggregates POC. This was not possible for the balanid nauplii experiments and we therefore used the fecal pellet production as an estimate for their grazing on aggregates (see section "Aggregate Feeding Rate" in the Results).

the amount of aggregated material which was added to each roller tank. To determine the initial POC concentrations of the added aggregates, the contents of five of the ten Petri dishes were filtered onto one pre-combusted GF/F filter and total POC concentration was measured on a GC elemental analyzer (see below). The photographs of the aggregates in the five Petri dishes that were filtered for POC were analyzed to calculate the total filtered aggregate volume. Hence, using the measured POC concentration and aggregate volumes, we determined the start POC to volume ratios of the incubated aggregates from which we calculated the start aggregate POC for each roller tank (**Table 3**). Note that the MSC collection did not contain enough *in situ* collected marine aggregates to measure the POC content of the aggregates added at the start of the incubation for balanid nauplii. We instead used the fecal pellet production to estimate their feeding rate on aggregates (see section "Aggregate Feeding Rate" in the Results). The roller tanks were incubated on a roller table that rotated with three rounds per min for >1 day in darkness at *in situ* temperature (0°C) (**Table 3**). The slow rotation speed of the roller table was adjusted to keep the aggregates in suspension and at the same time taking care not to disturb the zooplankton feeding behavior. At the end of the incubation we gently picked all copepods and balanid nauplii and ensured that they were alive before preservation in 4% formaldehyde solution for later genus and developmental stage identification. All visible aggregates from each roller tank were carefully transferred to a Petri dish using a wide-bore pipette. The remaining particles and fecal pellets were gently concentrated by gravity filtration through a 5 μm mesh. All fecal pellets were separated from the aggregates and particles. Both fecal pellets and aggregates were photographed to determine sizes and abundances. All collected aggregates from the five roller tanks for each incubation experiment were pooled and filtered onto one pre-combusted GF/F filter for later POC determinations. The POC to volume ratios were used to determine the amount of aggregate POC in each roller tank at the end of the incubation.

POC Determination

The filters with the pooled aggregates were dried at 40°C for 24 h, fumed with 37% HCL to remove inorganic carbon, and analyzed with a GC elemental analyzer (Elementar vario EL III, precision of ±0.7 μg C or ±0.3%) to obtain the total POC. We corrected for eventual contamination by measuring POC values of blank filters. Images of aggregates filtered at the start and end of the incubations were analyzed with the program ImageJ to determine the size of each individual aggregate. The images were converted into 8-bit, the background removed by duplicating the image and blurring the duplicate with a Gaussian Blur (200

pixel radius) before subtracting the duplicate from the original image. This created an even, dark background that was removed with a manual threshold of pixel-intensity 10, which identified all aggregates as objects that were having pixel-intensities brighter than 10. We calculated the equivalent spherical diameter (ESD) from the projected area of each aggregate. POC content per aggregate was calculated from their volumes using the measured POC to volume ratios determined at the start and at the end of the grazing incubations. Since marine snow aggregates have increasing porosities with increasing sizes, their size-specific POC content is best described by a power function $POC = a \times V^b$, where the POC content of an aggregate was in μg C, the aggregate volume V was in mm^3, b was fixed to 0.5, and a was a constant that was fitted to the volume of each aggregate so the sum of aggregate POC matched the measured POC for the pooled aggregates (after Alldredge, 1998, 2000; Alldredge et al., 1998; Ploug and Grossart, 2000). The volumetric POC relationship for the aggregates filtered at the start of the experiment was applied to aggregates added to the roller tanks to obtain the start aggregate POC concentration for each roller tank (POC_{start}). The volumetric POC relationship for the aggregates filtered at the end of the experiment was used to calculate the aggregate POC concentration at the end of the incubation (POC_{end}). Carbon ingestion from aggregate feeding was estimated by dividing the carbon loss per roller tank by the number of individual zooplankton in the roller tank and the incubation time.

Video Recordings

The video recordings were done in an aquarium (5 × 5 × 20 cm) with two Basler acA1300-30gc cameras (1 Mega-pixel, IR-filter removed) recording simultaneously from the front and left side of the aquarium. The aquarium was illuminated from the back and right side with two infrared-backlights (MBJ DBL plate, 880 nm, and custom-build plate with Vishay LEDs, 850 nm). This provided two camera views with back lighting from which we obtained 90° stereoscopic shadow images of the aggregates and copepods. One of the cameras was placed in a fixed position and used to determine the swimming speed of the copepods, and the size and sinking velocity of the settling aggregates. The other camera was attached to a stand that allowed movements in *x*-, *y*- and *z*- directions in order to keep individual aggregates in focus while they sank through the aquarium. Zoom and focus were kept constant for both cameras during the incubations to obtain a constant pixel-size of the recordings. All video recordings were done in darkness, with only infrared illumination, at *in situ* water temperature (0°C). The aquarium was filled with GF/F filtered seawater from the MSC. Copepods and balanid nauplii were allowed to acclimate in the aquarium for 1 h prior to filming. In order to ensure that enough individuals were in the middle of the aquarium (field of view of the camera), we added 30 balanid nauplii, 10 *Calanus* and 20 *Pseudocalanus* specimen, respectively. This was four-fold the concentration compared to the roller tank incubations (**Table 3**). However, we did not observe that the copepod or balanid nauplii abundances caused interactions and stress among the organisms during the incubations, and generally just a few of the individuals were in the middle of the aquarium simultaneously. Aggregates were first placed in a Petri dish containing seawater from the aquarium to ensure that the temperature and salinity of the pore water in the aggregates was similar to that in the aquarium. During a video sequence, one aggregate was gently transferred from the Petri dish to the aquarium with a wide bore-pipette. The aggregate was allowed to sink out of the pipette and into the aquarium. The aggregate was kept in focus during its descend through the aquarium. The aggregates ranged in size from 0.06 to 1.22 mm with settling velocities between 0.8 to 381 m d^{-1}. It typically took an aggregate 5 min to sink through the aquarium, whereafter the cameras and infrared lights were switched off for 5 min to minimize water heating and to dilute any chemical trails left in the wake of the previously recorded aggregate.

Video Analyses

In total 98, 73, and 65 individual aggregates were allowed to sink through the aquarium for feeding behavior investigations of *Calanus*, *Pseudocalanus*, and balanid nauplii, respectively. All video sequences were analyzed frame by frame to detect all zooplankton-aggregate interactions. We did not detect any encounters between balanid nauplii and aggregates during our video recordings (approximately a total of 5 h of video recordings). We identified four main responses upon encounters between copepods and sinking aggregates: attachment, avoidance, rejection and no reaction. Attachment was defined as a situation in which a copepod stayed attached to an aggregate for longer than 1 s. Rejection was defined when a copepod that attached to an aggregate for a period shorter than 1 s either detached from it or, for small aggregates, 'kicked' the aggregate away from its feeding appendages. Avoidance was defined when a copepod swam toward an aggregate but changed its swimming direction in the vicinity of the aggregate, seemingly to avoid encounter. No reaction was defined when a copepod was close to an aggregate without showing any visible reaction to the presence of the aggregate. This also included copepods that were swimming into an aggregate without altering swimming speed or direction and without attaching to the aggregate. For each response, the detection distance (distance at which a reaction was observed: <69 mm) and position of the copepod relative to the aggregate (above, below, beside) was recorded together with the impact of the encounter (e.g., whether the aggregate settling was altered or if the aggregate was fragmented). All events when aggregates were not within detection distance (>69 mm) of a copepod were defined as 'other.' Additionally, we recorded the duration of each attachment and any change in aggregate volume caused by the attachment. Aggregate sizes were determined by measuring the *x*- and *y*-axes of the aggregates in a video frame captured by the fixed camera. The shorter of the two axes was used as z-axis to calculate the volume of an aggregate assuming an ellipsoid form [Sun and Liu, 2003, Eq. (1)]. When possible, control measurements of the *z*-axes were done using the footage from the other camera, and a comparison of both methods showed good matches.

The aggregate volume (V, mm^3) was calculated using the x, y, and z lengths (mm), based on the following formula:

$$V = \frac{\pi}{6} xyz \quad (1)$$

The ESD was calculated from the aggregate volume as follows:

$$ESD = 2 \times \left(\frac{3}{4} V \times \frac{1}{\pi} \right)^{\frac{1}{3}} \quad (2)$$

Aggregate sinking velocity was determined using the fixed camera only, by analyzing the trajectory of the settling aggregate in ImageJ using the plugin MTrackJ. The length of the vertical trajectory was divided by the number of frames of the track and multiplied with the frame rate (frames s^{-1}) to obtain the sinking velocity. When possible, we determined aggregate volume and sinking velocity before the aggregates had encountered zooplankton.

Calculating *in situ* Zooplankton Aggregate Feeding

Zooplankton Abundance

We used a MultiNet (Midi, Hydro-Bios, Kiel) with nets of 200 μm mesh-size to determine the abundance of zooplankton in five depth-intervals in Erik Eriksen Strait (**Table 2**). Due to a malfunction of the MultiNet, a WP-2 net (200 μm mesh-size) without closing mechanism was used to determine zooplankton abundance in Hornsund and Storfjorden. Sampling was done in one vertical net haul, thus, the vertical distributions at these stations could not be determined. The flow-meter on the MultiNet showed that the filter-efficiency was 0.77 and we assumed that the WP-2 had a similar filter-efficiency. The MultiNet analyses showed that 72% of all *Calanus* and 69% of all *Pseudocalanus* resided in the upper 25 m. We therefore assumed that this was similar for the WP-2 nets from Hornsund and Storfjorden. All zooplankton samples were preserved in 4% formaldehyde solution buffered with Borax and analyzed in the home laboratory. Biomass was estimated using literature values for the dry weight of specific copepod developmental stages (Richter, 1994).

In situ Aggregate Size and Abundance

The vertical aggregate abundance and size-distribution was measured with an *in situ* camera system (ISC) in Hornsund, Storfjorden and Erik Eriksen Strait. The ISC is a camera system that is illuminated by an infrared backlight (Markussen et al., 2020). During our cruise, the ISC sampled a water volume of 20 ml every 15 cm during the down-cast. The pixel size was 24 μm, resulting in quantitative detection of particles that have ESDs > 100 μm. The ISC was connected to a SeaBird 19 CTD that was equipped with a fluorescence sensor. We processed the images with the Imaging Processing Toolbox in Matlab (The Mathworks) to characterize individual particles (see Markussen et al., 2020). The size of a particle was determined from its area and converted into ESD. Detected particles were sorted into logarithmically spaced size bins based on their ESDs. The concentration particle size spectra (n_C) were calculated for each size bin from the particle number concentration (ΔN_C) within a given size bin (Δd) for each water depth imaged:

$$n_c = \frac{\Delta N_C}{\Delta d} \quad [\#m^{-3}\ cm^{-1}] \quad (3)$$

We binned 10 images and obtained a vertical depth-resolution of ∼1.5 m.

POC Fluxes and Attenuation From Sediment Traps

We deployed drifting sediment traps in Hornsund and Erik Eriksen Strait. The sediment trap cylinders (KC Denmark A/S, Ø 7.2 cm, 45 cm long) were deployed at 20, 30, 40, 60, and 90 m in Hornsund and at 30, 40, 60, 90, 120, and 150 m depth in Erik Eriksen Strait. Each collection depth was equipped with four sediment trap cylinders. The deployment time was 20 h and 50 min in Hornsund and 23 h in Erik Eriksen Strait. We transferred the content from the four trap cylinders at each collection depth into a carboy immediately after recovery and stored the carboys at 0°C in darkness for a maximum of 6 h while filtrations for biogeochemical analyses were done. We subsampled the exported material from the carboys to determine POC fluxes from each collection depth. This was done by filtering the subsamples onto pre-combusted GF/F filters in triplicates within 6 h after the sediment trap array was retrieved. The filters were immediately frozen and stored at −20°C until arrival at the laboratory where the samples were dried for 48 h at 50°C, fumed with fuming HCl (37%) for 24 h to remove calcium carbonate, and analyzed with a GC elemental analyzer (Elementar vario EL III). We used the POC flux from 30 and 60 m (F_{30} and F_{60}, respectively) to calculate the fractional loss in carbon flux between the two depths. This was calculated by $1\text{-}F_{60}/F_{30}$. This approach assumes that the settling aggregates sank vertically through the water column and that the flux at 60 m was directly comparable to that at 30 m, i.e., vertical downward export.

Volumetric POC Relationships

We redeployed the traps at the same location immediately after each recovery of the first and long trap deployment in Hornsund and Erik Eriksen Strait. For the second trap deployment we only deployed two trap cylinders at each collection depth (20, 30, 40, 60, and 90 m). One trap cylinder at each depth was equipped with an insert cup that was filled with a viscous gel (TissueTek, OCT, cryogel from Sakura Finetek), which allowed preservation of size and three-dimensional structure of the aggregates collected in the gel trap (Wiedmann et al., 2014; Thiele et al., 2015; Flintrop et al., 2018). The second trap cylinder from each depth was used to collect biogeochemical fluxes, as described above. The second trap deployment lasted between 2 and 3 h to ensure that the settling aggregates did not overlap in the gel traps. After recovery, the content of the gel-free trap cylinder from each depth was transferred to one carboy and analyzed as described above. The gel traps were gently removed from the collection cylinder and frozen until imaging in the home laboratory. The images were analyzed as described in Wiedmann et al. (2014) to determine size, abundance, and

types of the collected particles and aggregates. We determined the size-specific POC content of the aggregates collected at each depth in the gel traps using a power function to relate the total POC content that was collected by the trap cylinder which was deployed simultaneously with the gel traps. The size-specific POC content was calculated by a power function $POC = a \times V^b$, where the POC content of an aggregate was in µg C, the aggregate volume V was in mm^3, b was fixed to 0.5, and a was a constant that was fitted to the volume of each aggregate collected in the gel traps. We adjusted a until the sum of aggregated POC from the gel traps matched the total measured POC collected by sediment trap cylinder. As there was no gel trap deployed in Storfjorden, we used the volumetric POC relationship of the MSC aggregates from the *Pseudocalanus* incubation, which was within the range of those determined for the gel traps.

POC Attenuation From ISC

We used the vertical particle size-distribution and abundance measured with the ISC to calculate POC concentration profiles for the size-range of aggregates that the ISC detected. This was calculated by applying the volumetric POC relationships, as determined from the gel trap deployments, to the different particle abundances for each size bin from the ISC, and summed the total POC concentrations from all size bins for each depth. To identify the depth interval in which the highest POC degradation took place, we plotted the POC concentration over depth and identified the depth range with the largest rate of change. This was identified from the POC peak (POC_{peak}, typically found between 5 and 20 m) and the depth where the rapid decline in POC concentrations ceased and the POC concentration became quasi constant with increasing depth (POC_{low}, typically 18 to 25 m below the depth of POC_{peak}). The fractional POC loss through this depth interval was calculated by 1-POC_{low}/POC_{peak}.

Encounter and Ingestion Rates

Encounter and ingestion rates for *Calanus* and *Pseudocalanus* were calculated as described in Koski et al. (2005) with slight adaptations, using parameters obtained from the incubations and video recordings (see units and values in **Table 4**). All ingestion rates were determined from the roller tank incubations while the copepod feeding behavior, encounter rate, detection distance, time a copepod spend on an aggregate, aggregate size-specific settling velocity, and copepod swimming speed were determined from the video recordings (**Table 4**). We did not observe any encounters between balanid nauplii and aggregates during the video recordings and, therefore, we only applied the following calculations to *Calanus* spp. and *Pseudocalanus* spp. The encounter kernel β describes the volume of water that a copepod can search per unit time for a given aggregate radius:

$$\beta(r) = v \times \pi \times \left(\frac{s}{2} \times l \times r\right)^2 \quad (4)$$

where v is the average swimming speed (including pause events), s is the total length of the copepod's first antenna, l is the detection distance at which the copepod can perceive a sinking aggregate, and r is the ESD radius of the sinking aggregate.

TABLE 4 | Parameters obtained from the experiments and *in situ* measurements used for calculating *in situ* aggregate feeding.

Parameter		Unit	*Calanus*	*Pseudocalanus*
Sinking velocity	sv	m d^{-1} (ESD:mm)	$48*ESD^{0.85}$	
Antenna length	h	mm	5.7	1.7
Detection distance	l	mm	0.69	0.69
Swimming velocity	v	mm s^{-1}	1.21	0.89
Fraction attachments	f		0.07	0.49
Time on aggregate	δ	s	35	12
Ingestion rate	i	µg C s^{-1} (r:mm)	$\frac{0.117}{1+e^{\frac{0.697-r}{0.161}}}$	$\frac{0.0322}{1+e^{\frac{0.379-r}{0.0966}}}$
POC content		µg C (vol:mm^3)		
Erik Eriksen St			$4.29*vol^{0.5}$	
Hornsund			$0.84*vol^{0.5}$	
Storfjorden			$3.19*vol^{0.5}$	

Sinking velocity was obtained from the video recordings of aggregates from Storfjorden, the length of the first antenna, detection distance, swimming velocity, the fraction of interactions that leads to an attachment, and the time spend on an aggregate were determined from the video recordings. The ingestion rates were fitted to the incubation experiments using the previous parameters. The POC content of an aggregate was determined from the sediment traps at Erik Eriksen St and Hornsund, and the MSC at Storfjorden.

Using β, the numbers of copepods that a sinking aggregate with radius r encounters during its descent through a water column of depth z is:

$$E(r) = \beta(r) \times C \times \frac{z}{u(r)} \quad (5)$$

where C is the average copepod concentration over depth z, and (ur) is the size-specific aggregate sinking velocity. The fractional degradation (κ) caused by copepod feeding of an aggregate that sinks to depth z is:

$$\kappa(r) = \frac{E(r) \times \alpha \times i \times \delta}{POC(r)} \quad (6)$$

where α is the fraction of encounters that lead to attachment, δ is the time a copepod spends on an aggregate, i is the carbon ingestion rate of a copepod when feeding on an aggregate and $POC(r)$ is the size-specific POC-content of the aggregate. All input parameters were directly obtained from the video recordings and the incubations. For δ we averaged the attachment times, as there was no relationship between aggregate size and time spend on the aggregate. We therefore assume that the ingestion (i) is a sigmoid function of aggregate size (since small aggregates contain little POC but can be ingested whole and ingestion per time on large aggregates reach a maximum independent on how much POC the aggregate contains):

$$i = \frac{a}{1 + e^{\frac{b-r}{c}}} \quad (7)$$

To fit the parameters a, b, and c for i, we first calculated i by assuming that κ was constant for different aggregate sizes and used the overall fractional degradation found from the roller tank incubations as a value for κ. We then fitted a sigmoid curve to the i values against aggregate sizes using the non-linear least-squares method in R (nls) and used the

resulting fit to determine the size-specific i for each of the investigated copepod species and aggregate types found at the three locations (Hornsund, Storfjorden, and Erik Eriksen Strait). In this way, Eq. (6) provided the total ingestion by copepods that a settling aggregate with a given radius would be exposed to as it sinks through a water depth with a known copepod concentration.

Calculating POC Attenuation by Zooplankton

Using the previously fitted parameters, the concentration of *Pseudocalanus* and *Calanus* in the upper 25 m, the depth interval z per ISC cast, and the POC_{peak} from the ISC casts, we calculated the *in situ* encounter kernel β, the number of encounters E, and the fraction degradation κ. The POC degradation per aggregate size-bin by each zooplankton (POC_{zoo}) is multiplied by the start POC (POC_{peak}) per size-bin. The fraction of POC that is degraded by zooplankton is:

$$\kappa_{tot} = 1 - \frac{\Sigma POC_{zoo}}{\Sigma POC_{peak}} \quad (8)$$

where both POC values are summed for all aggregate sizes (sum of all aggregate size-bins). We also estimated the microbial degradation, assuming the carbon-specific degradation is 0.03 d^{-1} (Morata and Seuthe, 2014; Belcher et al., 2016b):

$$\kappa_{micro}(r) = 1 - e^{-\frac{0.03}{u(r)} * z} \quad (9)$$

RESULTS

On-Board Experiments

Aggregate Feeding Rates

We performed aggregate feeding incubations with three dominant zooplankton representatives: copepods of the genera *Pseudocalanus* and *Calanus* and balanid nauplii at each of the three investigated regions: Hornsund, Erik Eriksen Strait, and Storfjorden, respectively (**Table 2**). The *Calanus* incubations were carried out with a mixture of different stages of *Calanus glacialis* and *Calanus hyperboreus* with an average prosome length of 3.08 ± 0.38 mm (SD, here and in the following text). *Pseudocalanus* incubations were carried out only using adult females with an average prosome length of 0.85 ± 0.08 mm (**Table 3**). Two species of the genus *Pseudocalanus* (*P. minutus* and *P. acuspes*) commonly occur in the regions studied, and their *in vivo* distinction is practically impossible. For this reason, it was assumed that the results of the incubation experiments should be treated as representative for genera and not specific species. When describing results we refer to *Calanus* or *Pseudocalanus*.

The average ingestion rate of *Calanus* was three times higher than that of *Pseudocalanus* (13.4 ± 4.34 and 5.79 ± 2.17 μg C ind^{-1} d^{-1}, respectively). We only had a limited number of collected aggregates for the balanid nauplii incubations, which were not enough to measure a start POC concentration (see section "Materials and Methods"). We therefore decided to estimate the ingestions from the fecal pellet numbers and sizes at the end of the experiments. However, the balanid nauplii only produced 1.5 fecal pellets ind^{-1} d^{-1} during the incubations and even when pooling all the pellets on one filter there was not enough material to be above the detection limit for the elemental analyzer. We measured the sizes of 27 of the produced pellets, which were on average 135 ± 31 μm long, with an average diameters of 71 ± 15 μm, resulting in an average volume of $3.9 \pm 1.9 \times 10^4$ mm^3, when using Eq. (1) to calculate the volume of an ellipsoid. We used POC to volume ratios of 80 μg C mm^{-3} for Arctic copepods provided by Reigstad et al. (2005) to estimate the POC content of the balanid fecal pellets. The average volume of a balanid fecal pellet was 0.0004 mm^3, which suggested that each pellet contained 0.03 μg C. A rough estimation of ingestion has traditionally assumed that one third is egested, one third used for growth and one third is respired (Kiørboe et al., 1985; Lenz et al., 1993; Båmstedt et al., 1999). Using those assumptions and the egestion rate of 1.5 fecal pellets ind^{-1} d^{-1} (0.05 ± 0.01 μgC ind^{-1} d^{-1}), we estimated that one balanid nauplii ingested 0.14 ± 0.02 μg C ind^{-1} d^{-1} during the aggregate grazing incubations (**Table 3**).

Aggregate Size, Sinking Velocity and Interactions

Aggregates used in the incubations with *Calanus* and *Pseudocalanus* were of similar size, with an average ESD of 0.35 ± 0.27 mm and 0.39 ± 0.28 mm, respectively (Wilcoxon rank sum test, p = 0.37). Aggregate sinking velocities measured during the experiment with *Calanus* were on average three-fold higher (92 ± 98 m d^{-1}, n = 98) than those measured during the experiments with *Pseudocalanus* (28 ± 25 m d^{-1}, n = 73), however, they were not significantly different (Spearman Rank Order Correlation, $p > 0.05$). The differences in the average sinking velocities was due to some large and fast-settling aggregates in the *Calanus* video incubations, which sank through the aquarium without being within detection distance of the copepods.

Copepod Feeding Behavior on Settling Aggregates

Pseudocalanus reacted to a higher fraction of the aggregates in its vicinity (within detection distance) than *Calanus*, and only 6% of the aggregates that were within 0.5 body-length from *Pseudocalanus* did not cause a behavioral response, compared to 48% for *Calanus* (**Supplementary Video 1**). We observed two clear ingestion events for *Calanus* (reaction to 7% of the aggregates in their vicinity) with one event involving a small slow-sinking aggregate (ESD 0.1 mm, SV 5.9 m d^{-1}) and one event involving a larger aggregate (ESD 0.3 mm, SV 58 m d^{-1}, **Supplementary Video 2**). During these two events *Calanus* attached to the aggregates for 2.3 s and 67.5 s, respectively. Four attachments resulted in rejections within 1 s after attaching. In these cases aggregate ESDs ranged between 0.15 and 0.22 mm and the aggregates sank with velocities between 3 and 17 m d^{-1} (**Supplementary Video 3**). Seven aggregates were actively avoided, of which four had sinking velocities higher than 100 m d^{-1}. In contrast, *Pseudocalanus* attached more frequently to aggregates, with 26 recorded attachments. Here aggregate ESDs ranged between 0.06 and 0.83 mm and sinking velocities were between 0.8 and 58 m d^{-1} (**Supplementary Video 4**). The average attachment time was 12 ± 14.5 s (range: 1 to 66 s). *Pseudocalanus* actively avoided 21 aggregates, with ESDs ranging

between 0.1 and 1.22 mm and sinking velocities between 2.7 and 96 m d^{-1} (**Supplementary Video 5**). Four aggregates were rejected directly upon attachment, with ESDs ranging between 0.04 and 0.55 mm and sinking velocities between 3 and 48 m d^{-1}.

Detection Distance

The two observed *Calanus* attachments were established by copepods that approached the aggregate from the side, and detected the aggregate at a distance of 0.69 ± 0.08 mm (**Supplementary Video 2**, **Figure 2**). The aggregates that were avoided (**Supplementary Video 3**, **Figure 2**) were in a similar proximity (0.67 ± 0.63 mm), although when the copepod was swimming above the sinking aggregate this distance was slightly larger (0.95 ± 0.69 mm). We observed *Calanus* to encounter aggregates during swimming events without capturing the aggregates, however, some of these encounters fragmented the aggregates. Most of the *Pseudocalanus* attachments occurred during filter feeding events while the aggregate sank into the feeding current from above, whereupon the filter feeding activity would be interrupted and the copepod would capture and attach to the aggregate by grapping it with the mandibles (**Supplementary Video 4**, **Figure 2**). The average detection distance for these events was 0.46 ± 0.40 mm, whereas the detection distance for copepods that approached aggregates from above or aside was 1.08 ± 0.85 mm and 0.78 ± 0.43 mm, respectively. Avoidance events occurred within similar reaction distances as those observed for the attachment events. One exception occurred when a copepod swam 13.4 mm above the aggregate and followed the track of the sinking aggregate (likely following the chemical trail at the wake of the aggregate) but avoided it from a distance of 0.96 mm (ESD 0.81, SV 84 m d^{-1}) (**Supplementary Video 5**, **Figure 2**). Additionally, four aggregates were rejected within 1 s upon attachment.

In situ Zooplankton Aggregate Feeding

Zooplankton Abundances

The total copepod abundance was the highest in Erik Eriksen Strait and the lowest in Hornsund (**Table 2**). Calanoid nauplii contributed 83% to the total zooplankton abundance in Erik Eriksen Strait, balanid nauplii contributed 28% to the total zooplankton abundance at Hornsund, and nauplii from copepods and balanid contributed 91% to the total zooplankton abundance in Storfjorden (**Table 2**). Combined *Calanus* spp. and *Pseudocalanus* spp. contributed to the total zooplankton abundance with 13%, 53%, and 6% in Erik Eriksen Strait, Hornsund, and Storfjorden, respectively (**Table 2**). *Calanus* abundances in the upper 25 m (NB: only Erik Eriksen Strait were sampled with MultiNet while the other two were sampled with WP-2 in the full water column – see "Materials and Methods") were 120, 498, and 289 ind. m^{-3}, *Pseudocalanus* abundances were 185, 27, and 183 ind. m^{-3}, and balanid nauplii abundances were 161, zero, and 2686 ind. m^{-3} in Hornsund, Erik

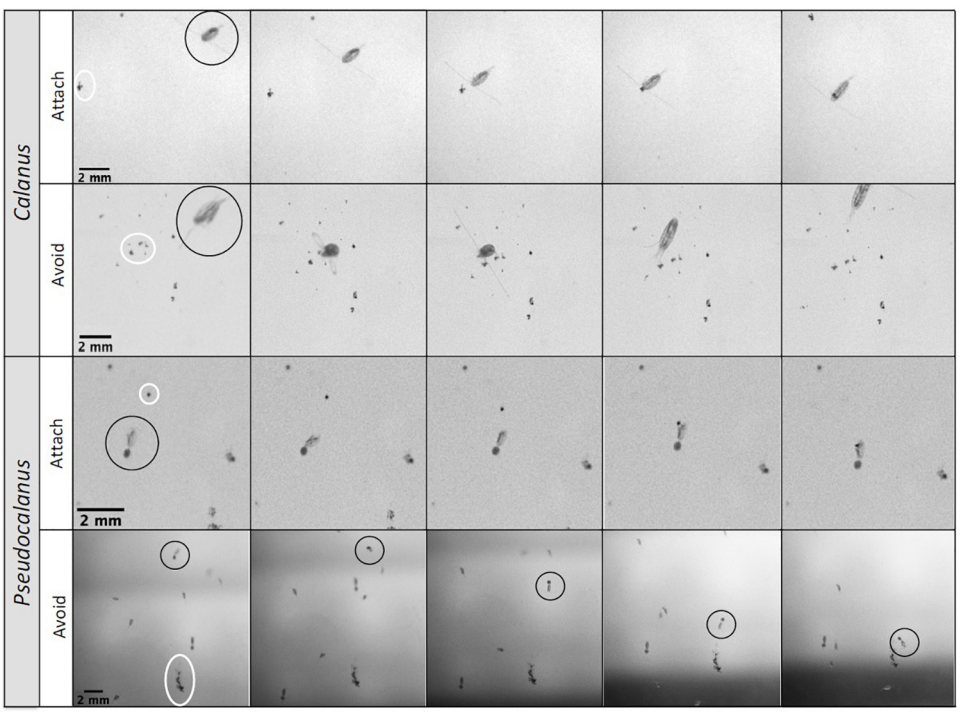

FIGURE 2 | Stills from videos with interactions between copepods (marked with black circles) and sinking aggregates (marked with white circles). ***Calanus* Attach:** *Calanus* spp. swims from the side toward an aggregate and attaches to it. ***Calanus* Avoid:** *Calanus* spp. swims, changes course, touches an aggregate with its swimming legs (3rd photo), and jumps away. ***Pseudocalanus* Attach:** *Pseudocalanus* spp. female is filter feeding, jumps, swims toward the sinking aggregate, attaches to the aggregate with its swimming legs, and sinks while feeding. ***Pseudocalanus* Avoid:** *Pseudocalanus* spp. (circle) swims back and forth 13 mm above a sinking aggregate, follows its trail down, but swims away from the aggregate when in the vicinity.

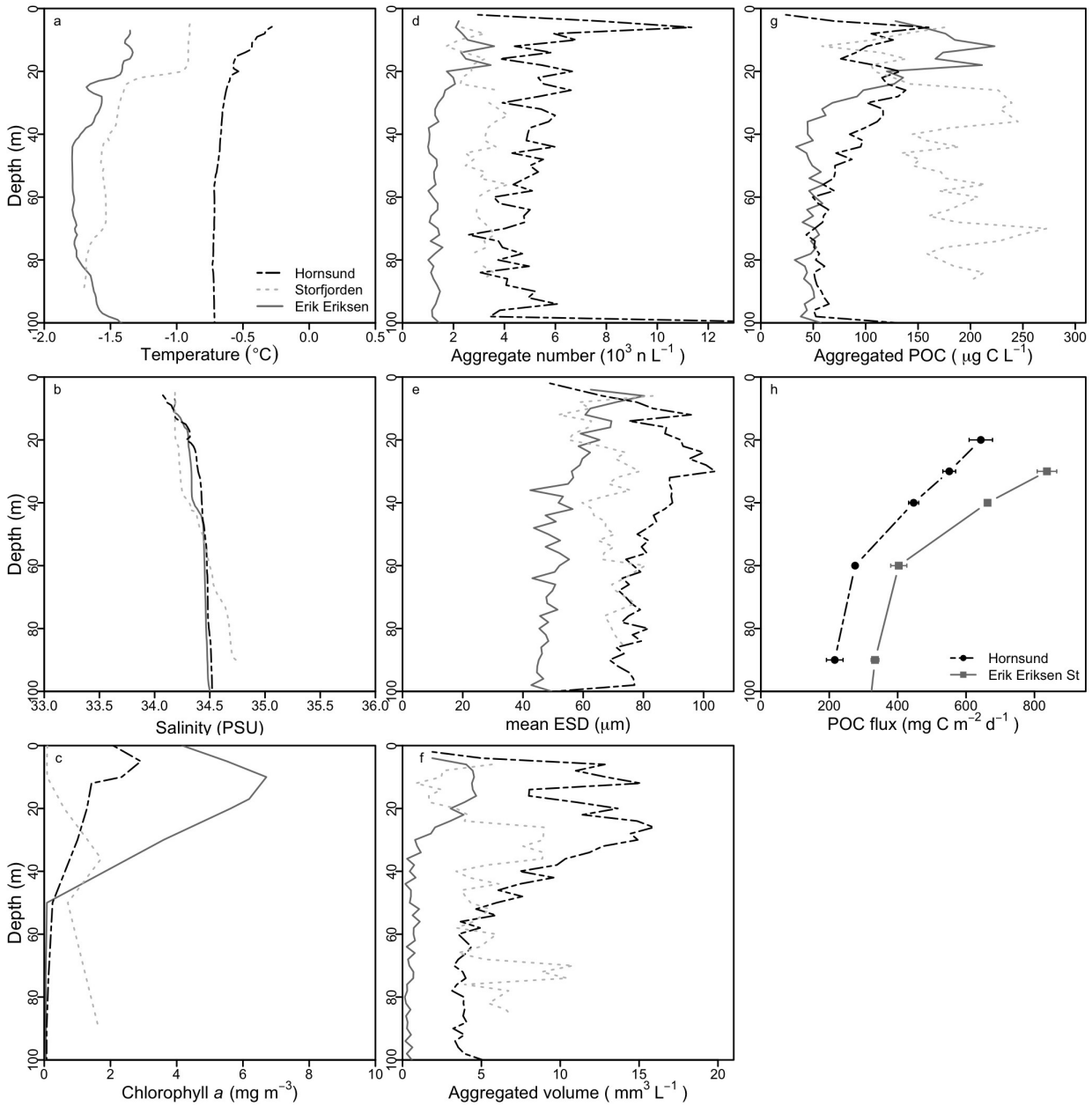

FIGURE 3 | Averaged depth profiles for investigated properties for measurements from stations in Erik Eriksen Strait (averaged values for five measurements), in Hornsund (averaged values for six measurements) and in Storfjorden (only one measurement), and POC fluxes from the sediment traps. **(a)** Temperature, **(b)** salinity, **(c)** chlorophyll *a*, **(d)** number of aggregates, **(e)** mean equivalent spherical diameter (ESD), **(f)** total aggregate volume, **(g)** total aggregated particulate organic carbon (POC), and **(h)** POC fluxes from sediment traps (average ± sd).

Eriksen Strait, and Storfjorden, respectively. In terms of biomass, however, *Pseudocalanus* and *Calanus* dominated the zooplankton community at all three stations with 94%, 95%, and 85% of the total zooplankton biomass in Hornsund, Erik Eriksen Strait, and Storfjorden, respectively.

Aggregate Abundances and Flux Attenuation

We determined *in situ* aggregate abundance and size-distribution from 12 vertical profiles with the ISC. The total number of aggregates, the mean aggregate size, and the total aggregated volume was the highest in Hornsund, followed by Storfjorden, and the lowest in Erik Eriksen Strait, however, the highest POC concentrations in the upper 25 m was found in Erik Eriksen Strait while Storfjorden had the highest POC concentrations at depths below 25 m (**Figure 3**). We used the volumetric POC ratios to convert the total aggregated volume into total aggregated POC concentrations. At all three stations this showed a decrease in the POC concentration from the peak concentration down to 50 m:

by 46 ± 16% (number of profiles $n = 6$) at Hornsund, by 39% at Storfjorden ($n = 1$), and by 55 ± 21% at Erik Eriksen Strait ($n = 5$). POC flux collected by the free-drifting sediment traps was higher at Erik Eriksen Strait compared to Hornsund (**Figure 3h**), and the flux attenuation between 30 and 60 m, calculated based on these measurements was 58 and 50%, respectively (**Figure 4**).

In situ Aggregate Feeding

Compared to the POC flux attenuation determined from the sediment trap measurements (see above), the attenuation estimated based *in situ* camera profiles was 55 ± 21%, 46 ± 16%, and 39% at Erik Eriksen Strait, Hornsund, and Storfjorden, respectively (**Figure 4**). We used Eqs (3–8) to test the potential contribution from aggregate feeding by *Calanus* and *Pseudocalanus* to the observed POC flux attenuation. Based on these calculations *Calanus* aggregate feeding alone could account for 38–62% of the total observed POC attenuation at all three stations while *Pseudocalanus* feeding could account for 1.5–29% of the total observed POC attenuation. Assuming that microbes have a carbon-specific degradation of 0.03 d^{-1} in the polar waters (Morata and Seuthe, 2014; Belcher et al., 2016b), Eq. (9) suggested that microbial degradation accounted for 12–16% of the total observed POC flux attenuation at the three stations. When combining *Calanus* and *Pseudocalanus* feeding on settling aggregates with microbial degradation, we could explain 76%, 77%, and 77% of the total POC flux attenuation at Hornsund, Erik Eriksen Strait, and Storfjorden, respectively. The observed POC attenuation between the sediment traps at 30 and 60 m was 276 and 436 mg C m^{-2} d^{-1} in Hornsund and Erik Eriksen Strait, respectively. *Calanus* aggregate feeding was found to reach 102 and 269 mg C m^{-2} d^{-1} in Hornsund and Erik Eriksen Strait, respectively, while *Pseudocalanus* had a carbon-equivalent aggregate feeding of 76 and 6.3 mg C m^{-2} d^{-1} in Hornsund and Erik Eriksen Strait, respectively. Potential aggregate feeding by the balanid nauplii only accounted for 0.24 to 0.58% of the total observed flux attenuation at the three investigated regions.

Size-Specific Aggregate-Loss in the Upper 50 m

Compared to the observed POC concentration at 50 m from the ISC profiles, our calculations showed a stronger decline in the abundance of small aggregates and only a limited decline in the abundance of large aggregates (**Figure 5**). Still, the calculations clearly suggested that primarily zooplankton grazing and to some extent microbial degradation of small slow-sinking aggregates (ESD < 0.2 mm) accounted for the majority of the observed POC flux attenuation.

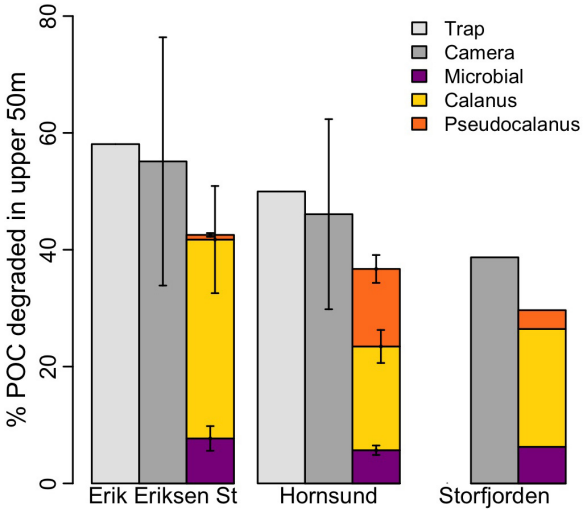

FIGURE 4 | POC degradation in the upper 50 m estimated based on measurements from drifting sediment traps (light gray), from camera profiles (dark gray), calculated microbial degradation based on a C-specific degradation of 0.03 d^{-1} (magenta), and calculated *Calanus* (yellow) and *Pseudocalanus* degradation (orange).

DISCUSSION

Our study showed that the majority of the POC flux attenuation in an Arctic shelf sea during the productive season took place in the upper 50 m of the water column. Attenuation processes are still under debate, e.g., the importance of microbial degradation versus zooplankton grazing and fragmentation, but evidence is increasingly showing that zooplankton play a major role in flux attenuation in the upper ocean (Iversen et al., 2010; Jackson and Checkley, 2011; Möller et al., 2012). *Calanus* spp. and *Pseudocalanus* spp. are important copepods and often dominate the zooplankton biomass in Arctic waters (Basedow et al., 2018; Carstensen et al., 2019), yet little is known about their contribution to POC flux attenuation. We observed that representatives of both *Calanus* and *Pseudocalanus* were able to detect, capture and feed on sinking aggregates. Both copepods were observed to attach to aggregates that were within a distance of half a body length, suggesting that they were detecting hydromechanical signals generated by the sinking aggregates (Visser, 2001). Additionally, it appeared that *Pseudocalanus* individuals were able to detect chemical trails from dissolved compounds leaking out of the sinking aggregates (**Supplementary Video 4**), a trait that has previously only been observed for the copepod *Temora longicornis* (Lombard et al., 2013). This detection did not, however, lead to aggregate capture. *Pseudocalanus* only captured aggregates that they detected via hydrodynamic signals. The results of this study suggest that the main mechanisms used to detect settling aggregates are based on hydromechanical signals in both *Calanus* and *Pseudocalanus*. While there were some instances where it seemed as though aggregates were detected via chemoreception, the recorded instances were too few to make any firm conclusion about the role of this mechanism for these two calanoid copepod genera.

Pseudocalanus attached more often to the encountered aggregates than *Calanus*. However, the larger size and higher swimming velocity resulted in a larger volume of water searched per time for an individual *Calanus* compared to an individual *Pseudocalanus*. Consequently, the probability of finding an aggregate was higher for individual *Calanus* compared to individual *Pseudocalanus*. Additionally, *Calanus* spent more

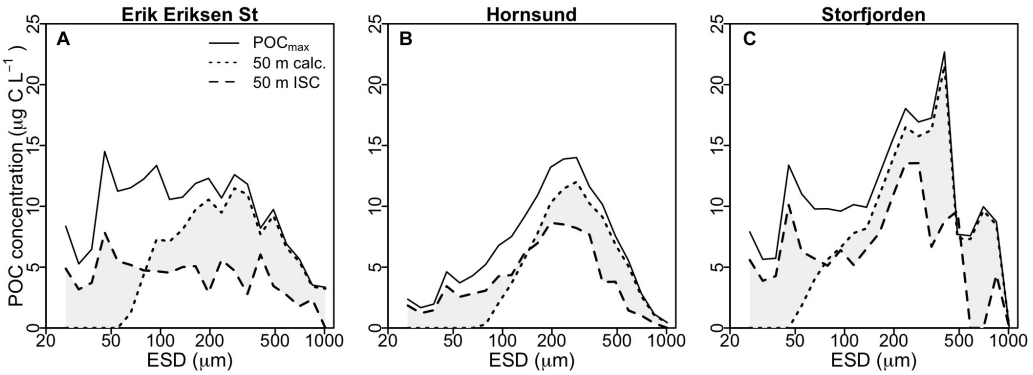

FIGURE 5 | Average POC distribution for different particle size classes at Erik Eriksen Strait **(A)**, Hornsund **(B)**, and Storfjorden **(C)**. Continuous lines show the POC_{max} values from the ISC profiles, used as input in the calculations, dotted black lines show the calculated values at 50 m, based on microbial degradation and *Calanus* and *Pseudocalanus* aggregate feeding, and black dashed lines show the measured values at 50 m from the ISC profiles. Gray shaded area indicates differences between observed and calculated POC concentration at 50 m.

time attached to an aggregate than *Pseudocalanus* and each *Calanus* ingested three-fold more aggregated POC than each *Pseudocalanus* (average aggregate ingestion was 13.4 ± 4.34 and 5.79 ± 2.17 µg C ind^{-1} d^{-1} for *Calanus* and *Pseudocalanus*, respectively). This is within previously reported grazing rates for these genera (Koski et al., 1998; Seuthe et al., 2007; Grote et al., 2015). Put in relation to the copepod carbon content (∼128 and ∼9 µg C ind^{-1} for *Calanus* and *Pseudocalanus*, respectively (Debes et al., 2008; Swalethorp et al., 2011), the carbon-specific ingestion rates for *Calanus* and *Pseudocalanus* were 0.12 ± 0.05 and 0.64 ± 0.24 d^{-1}, respectively. This is in the upper range of carbon-specific ingestion rates observed previously for those genera (Mayor et al., 2006; Arendt et al., 2010; Alcaraz et al., 2014) and it therefore seems possible that both species can sustain their carbon demand via aggregate feeding alone. While these calculations should be viewed as estimates, our direct video observations provide evidence that both *Calanus* and *Pseudocalanus* perceive settling aggregates as a food source.

The ecological impact of the two genera depends on their quantitative contribution to the zooplankton community in a given location. By combining aggregate ingestion rates of zooplankton with zooplankton abundance from net hauls and *in situ* abundance and size distribution of aggregates at the study location, we calculated that aggregate grazing by local populations of *Calanus* and *Pseudocalanus* could be responsible for 38 to 62% and 1.5 to 29%, respectively, of the total POC flux attenuation. Microbial respiration associated with the aggregates could account for a further 12–16% of the flux attenuation, when assuming an aggregate carbon-specific microbial degradation of 0.03 d^{-1}, as previously measured for aggregates from polar seas (Morata and Seuthe, 2014; Belcher et al., 2016b). Hence, combining aggregate feeding by *Calanus* and *Pseudocalanus* with microbial degradation explained as much as 77% of the total POC flux attenuation in the upper 50 m of the water column.

The remaining ∼23% of the flux attenuation can possibly be attributed to other zooplankton, nekton, and physical disturbances. The most abundant zooplankton groups at the three stations were balanid nauplii and calanoid nauplii, although they contributed little to the total zooplankton biomass due to their small sizes. Estimations from our incubations carried out with the balanid nauplii suggested that they only contributed of up to 0.58% of the total observed POC flux attenuation, despite their high abundance. Of the remaining observed zooplankton in the net hauls, only calanoid nauplii (Green et al., 1992), *Microsetella norvegica* (Koski et al., 2005, 2007), *Oncaea* spp. (Green and Dagg, 1997; Koski et al., 2017), and euphausiids (Dilling et al., 1998) have previously been observed to feed on sinking aggregates. Using published aggregate ingestion rates, euphausiids may have contributed 0.14–5.9% to the flux attenuation (Dilling et al., 1998), and small copepods, such as *Oncaea* spp. and *Oithona* spp., may have contributed <0.01–1.6%, assuming an aggregate ingestion rate of 1.08 µg C ind^{-1} d^{-1} (Kiørboe, 2000). Additionally, we observed dinoflagellates, which may also feed on settling aggregates (Poulsen and Iversen, 2008; Poulsen et al., 2011; Svensen et al., 2012). However, even combined, the contribution of zooplankton groups other than *Calanus* and *Pseudocalanus* is unlikely to alone explain the remaining 23%.

Another mechanism which may explain part of the remaining ∼23% of the POC flux attenuation is aggregate fragmentation, which has previously been suggested as a major process controlling the export of organic matter (Dilling and Alldredge, 2000; Goldthwait et al., 2004; Briggs et al., 2020). Fragmentation may increase the residence time of the settling aggregates in the upper water column by disaggregating them into smaller, slower-settling aggregates. This allows more time for microbial degradation (Iversen and Ploug, 2010; van der Jagt et al., 2018) and grazing by zooplankton (Iversen and Poulsen, 2007; Poulsen and Iversen, 2008; Giering et al., 2014; Mayor et al., 2014), thus decreasing the efficiency of the biological carbon pump. It has to be noted that encounters between zooplankton and settling aggregates may lead to aggregate fragmentation as well as aggregate feeding. This has been shown for *Calanus*, *Pseudocalanus*, and euphausiids (Dilling and Alldredge, 2000; Iversen and Poulsen, 2007). The major fragmentation mechanism, however, is likely aggregate break-up due to physical

forces in the upper water column (e.g., turbulence) (Jackson et al., 1995; Ruiz, 1997). We found that the modeled size-spectra (**Figure 5**) underestimated the *in situ* abundance of small aggregates and overestimated the abundance of large aggregates. This suggests that, while our calculations do include zooplankton activities, they are missing the physical aggregate fragmentation that converts large aggregates into small fragments. The main reason for this shortfall, is that our experimental setup (roller tanks), on which the model is based, did not allow for turbulence or other physical disturbances in the water. Hence, physical aggregate fragmentation may have been an important mechanism for *in situ* flux attenuation during our study and would explain the discrepancy between our calculated and observed POC size spectra at 50 m and potentially be the explanation for the additional ∼23% flux attenuation.

Polar marine environments are characterized by high primary production and high export flux out of the upper mixed layer, but strong POC flux attenuation at the base of the mixed layer (Berelson, 2001; Wassmann et al., 2003). Here we show that *Calanus* and *Pseudocalanus* were responsible for 60–67% of the flux attenuation. Both genera are ubiquitous in productive temperate and subtropical environments (Boxhall, 2001), which exhibit similar patterns of flux attenuation (e.g., Martin et al., 1983; Iversen et al., 2010; Belcher et al., 2016a). Currently, receding sea-ice cover and inflow of warm Atlantic water are leading to dramatic changes in the Arctic pelagic ecosystem. For example, environmental changes promote small flagellates (Li et al., 2009) and boreal zooplankton may be expatriated into the Arctic, replacing large Arctic species with smaller species of Atlantic origin (Hirche and Kosobokova, 2007). With the currently available data, it is difficult to predict how these changes at the base of the food web will impact the flux attenuation. Our study, however, confirms the suggestion by Jackson and Checkley (2011) that zooplankton may act as gatekeepers of the POC flux. In a future Arctic, where small copepods species with low impact on the attenuation prevail, carbon export may increase. It is, however, also possible that the shift from diatoms to flagellates will decrease the settling velocities of the formed aggregates (Ploug et al., 2008b) and thereby decrease carbon export and the efficiency of the biological carbon pump. This study shows that zooplankton feeding on aggregates can be an important attenuation mechanism in the Arctic. This highlights the necessity to understand the seasonal and regional role of zooplankton for both export and carbon flux attenuation and how future changes in Arctic trophic interactions and particle flux will alter ecosystem functions and services.

DATA AVAILABILITY STATEMENT

The original contributions presented in the study are included in the article/**Supplementary Material**, further inquiries can be directed to the corresponding author.

AUTHOR CONTRIBUTIONS

MI and HJ designed the experiments. HJ, IW, and MI did the measurements during the cruise. NH and BN counted and identified the zooplankton plankton samples. HJ, IW, NH, BN, and MI analyzed the data. HJ and MI wrote the manuscript with input from NH, IW, and BN. All authors contributed to the article and approved the submitted version.

FUNDING

The cruise and IW were funded by 'ARCEx' (Norwegian Research Council #228107 and industry partners). This study was supported by the Helmholtz Association, the Alfred Wegener Institute Helmholtz Centre for Polar and Marine Research and the DFG-Research Center/Cluster of Excellence "The Ocean in the Earth System" at MARUM. This publication was supported by the HGF Young Investigator Group SeaPump "Seasonal and regional food web interactions with the biological pump": VH-NG-1000.

ACKNOWLEDGMENTS

We thank Cindy Lee, Stuart Wakeham, Kai-Uwe Hinrichs, Carol Arnosti, Anne Pearson, and Thorsten Dittmar for organizing the Marine Organic Biogeochemistry workshop held at the Hanse-Wissenschaftskolleg, Delmenhorst, Germany, April 27 to 30th 2019. We thank Christiane Lorenzen for the POC measurements and the crew of the R/V Helmer Hanssen for assistance during the cruise. We thank the editor and three reviewers for valuable input.

SUPPLEMENTARY MATERIAL

The Supplementary Material for this article can be found online at: https://www.frontiersin.org/articles/10.3389/fmars.2020.543124/full#supplementary-material

REFERENCES

Alcaraz, M., Felipe, J., Grote, U., Arashkevich, E., and Nikishina, A. (2014). Paper II Life in a warming ocean: thermal thresholds and metabolic balance of Arctic zooplankton. *J. Plankton Res.* 36, 3–10. doi: 10.1093/plankt/fbt111

Alldredge, A. (1998). The carbon, nitrogen and mass content of marine snow as a function of aggregate size. *Deep. Res. I* 45, 529–541. doi: 10.1016/s0967-0637(97)00048-4

Alldredge, A. L. (1972). Abandoned larvacean houses: a unique food source in the pelagic environment. *Science* 177, 885–887. doi: 10.1126/science.177.4052.885

Alldredge, A. L. (2000). Interstitial dissolved organic carbon (DOC) concentrations within sinking marine aggregates and their potential contribution to carbon flux. *Limnol. Oceanogr.* 45, 1245–1253. doi: 10.4319/lo.2000.45.6.1245

Alldredge, A. L., Passow, U., and Haddock, S. H. D. (1998). The characteristics and transparent exopolymer particle (TEP) content of marine snow formed from thecate dinoflagellates. *J. Plankton Res.* 20, 393–406. doi: 10.1093/plankt/20.3.393

Arendt, K. E., Nielsen, T. G., Rysgaard, S., and Tönnesson, K. (2010). Differences in plankton community structure along the Godthåbsfjord, from the Greenland

Ice Sheet to offshore waters. *Mar. Ecol. Prog. Ser.* 401, 49–62. doi: 10.3354/meps08368

Arnkværn, G., Daase, M., and Eiane, K. (2005). Dynamics of coexisting *Calanus finmarchicus*, *Calanus glacialis* and *Calanus hyperboreus* populations in a high-Arctic fjord. *Polar Biol.* 28, 528–538. doi: 10.1007/s00300-005-0715-8

Båmstedt, U., Nejstgaard, J. C., Solberg, P. T., and Høisoeter, T. (1999). Utilisation of small-sized food algae by *Calanus finmarchicus* (Copepoda, Calanoida) and the significance of feeding history. *Sarsia* 84, 19–38. doi: 10.1080/00364827.1999.10420449

Basedow, S. L., Sundfjord, A., von Appen, W. J., Halvorsen, E., Kwasniewski, S., and Reigstad, M. (2018). Seasonal variation in transport of zooplankton into the arctic basin through the Atlantic Gateway, Fram Strait. *Front. Mar. Sci.* 5:194. doi: 10.3389/fmars.2018.00194

Belcher, A., Iversen, M., Giering, S., Riou, V., Henson, S. A., Berline, L., et al. (2016a). Depth-resolved particle-associated microbial respiration in the north-east Atlantic. *Biogeosciences* 13, 4927–4943. doi: 10.5194/bg-13-4927-2016

Belcher, A., Iversen, M., Manno, C., Henson, S. A., Tarling, G. A., and Sanders, R. (2016b). The role of particle associated microbes in remineralization of fecal pellets in the upper mesopelagic of the Scotia Sea, Antarctica. *Limnol. Oceanogr.* 61, 1049–1064. doi: 10.1002/lno.10269

Berelson, W. M. (2001). The flux of particulate organic carbon into the ocean interior: a comparison of four U S. JGOFS regional studies. *Oceanography* 14, 59–67. doi: 10.5670/oceanog.2001.07

Boxhall, G. (2001). "Copepoda (excl. harpacticoida)," in *European Register of Marine Species: A Check-List of the Marine Species in Europe and a Bibliography of Guides to Their Identification. Collection Patrimoines Naturels*, eds M. J. Costello, C. Emblow, and R. J. White (Paris: Meséum Naitonal d'Histoire Naturelle), 252–268.

Briggs, N., Dall'Olmo, G., and Claustre, H. (2020). Major role of particle fragmentation in regulating biological sequestration of CO2 by the oceans. *Science* 367, 791–793. doi: 10.1126/science.aay1790

Buesseler, K. O., and Boyd, P. (2009). Shedding light on processes that control particle export and flux attenuation in the twilight zone of the open ocean. *Limnol. Ocean.* 54, 1210–1232. doi: 10.4319/lo.2009.54.4.1210

Busch, K., Endres, S., Iversen, M. H., Michels, J., Nöthig, E.-M., and Engel, A. (2017). Bacterial colonization and vertical distribution of marine gel particles (TEP and CSP) in the Arctic Fram Strait. *Front. Mar. Sci.* 4:166. doi: 10.3389/fmars.2017.00166

Carstensen, J., Olszewska, A., and Kwasniewski, S. (2019). Summer mesozooplankton biomass distribution in the West Spitsbergen current (2001–2014). *Front. Mar. Sci.* 6:202. doi: 10.3389/fmars.2019.00202

Debes, H., Eliasen, K., and Gaard, E. (2008). Seasonal variability in copepod ingestion and egg production on the Faroe shelf. *Hydrobiologia* 600, 247–265. doi: 10.1007/s10750-007-9238-3

DeVries, T., Primeau, F., and Deutsch, C. (2012). The sequestration efficiency of the biological pump. *Geophys. Res. Lett.* 39:L13601. doi: 10.1029/2012GL051963

Dilling, L., and Alldredge, A. L. (2000). Fragmentation of marine snow by swimming macrozooplankton: a new process impacting carbon cycling in the sea. *Deep. Res. I* 47, 1227–1245. doi: 10.1016/s0967-0637(99)00105-3

Dilling, L., and Brzezinski, M. A. (2004). Quantifying marine snow as a food choice for zooplankton using stable silicon isotope tracers. *Plankton J. Res.* 26, 1105–1114. doi: 10.1093/plankt/fbh103

Dilling, L., Wilson, J., Steinberg, D., and Alldredge, A. (1998). Feeding by the euphausiid Euphausia pacifica and the copepod *Calanus pacificus* on marine snow. *Mar. Ecol. Prog. Ser.* 170, 189–201. doi: 10.3354/meps170189

Flintrop, C. M., Rogge, A., Miksch, S., Thiele, S., Waite, A. M., and Iversen, M. H. (2018). Embedding and slicing of intact *in situ* collected marine snow. *Limnol. Oceanogr. Methods* 16, 339–355. doi: 10.1002/lom3.10251

Giering, S. L. C., Sanders, R., Lampitt, R. S., Anderson, T. R., Tamburini, C., and Boutrif, M. (2014). Reconciliation of the carbon budget in the ocean's twilight zone. *Nature* 507, 480–483. doi: 10.1038/nature13123

Goldthwait, S., Yen, J., Brown, J., and Alldredge, A. (2004). Quantification of marine snow fragmentation by swimming euphausiids. *Limnol. Oceanogr.* 49, 940–952. doi: 10.4319/lo.2004.49.4.0940

Green, E. P., and Dagg, M. J. (1997). Mesozooplankton associations with medium to large marine snow aggregates in the northern Gulf of Mexico. *Plankton J. Res.* 19, 435–447. doi: 10.1093/plankt/19.4.435

Green, E. P., Harris, R. P., and Duncan, A. (1992). The production and ingestion of faecal pellets by nauplii of marine calanoid copepods. *J. Plankton Res.* 14, 1631–1643. doi: 10.1093/plankt/14.12.1631

Grote, U., Pasternak, A., Arashkevich, E., Halvorsen, E., and Nikishina, A. (2015). Thermal response of ingestion and egestion rates in the Arctic copepod *Calanus glacialis* and possible metabolic consequences in a warming ocean. *Polar Biol.* 38, 1025–1033. doi: 10.1007/s00300-015-1664-5

Hirche, H. J., and Kosobokova, K. (2007). Distribution of *Calanus finmarchicus* in the northern North Atlantic and arctic ocean-expatriation and potential colonization. *Deep Res. Part II Top. Stud. Oceanogr.* 54, 2729–2747. doi: 10.1016/j.dsr2.2007.08.006

Iversen, M. H., Nowald, N., Ploug, H., Jackson, G. A., and Fischer, G. (2010). High resolution profiles of vertical particulate organic matter export off Cape Blanc, Mauritania: degradation processes and ballasting effects. *Deep Res. Part I Oceanogr. Res. Pap.* 57, 771–784. doi: 10.1016/j.dsr.2010.03.007

Iversen, M. H., Pakhomov, E. A., Hunt, B. P. V., van der Jagt, H., Wolf-Gladrow, D., and Klaas, C. (2017). Sinkers or floaters? Contribution from salp pellets to the export flux during a large bloom event in the Southern Ocean. *Deep Sea Res. Part II Top. Stud. Oceanogr.* 138, 116–125. doi: 10.1016/j.dsr2.2016.12.004

Iversen, M. H., and Ploug, H. (2010). Ballast minerals and the sinking carbon flux in the ocean: carbon-specific respiration rates and sinking velocities of marine snow aggregates. *Biogeosciences* 7, 2613–2624. doi: 10.5194/bg-7-2613-10

Iversen, M. H., and Ploug, H. (2013). Temperature effects on carbon-specific respiration rate and sinking velocity of diatom aggregates - potential implications for deep ocean export processes. *Biogeosciences* 10, 4073–4085. doi: 10.5194/bg-10-4073-2013

Iversen, M. H., and Poulsen, L. K. (2007). Coprorhexy, coprophagy, and coprochaly in the copepods *Calanus helgolandicus*, *Pseudocalanus elongatus*, and *Oithona similis*. *Mar. Ecol. Prog. Ser.* 350, 79–89. doi: 10.3354/meps07095

Jackson, G. A. (1993). Flux feeding as a mechanism for zooplankton grazing and its implications for vertical particulate flux. *Limnol. Oceanogr.* 38, 1328–1331. doi: 10.4319/lo.1993.38.6.1328

Jackson, G. A., and Checkley, D. M. Jr. (2011). Particle size distributions in the upper 100 m water column and their implications for animal feeding in the plankton. *Deep Res. I* 58, 283–297. doi: 10.1016/j.dsr.2010.12.008

Jackson, G. A., Logan, B. E., Alldredge, A. L., and Dam, H. G. (1995). Combining particle size spectra from a mesocosm experiment measured using photographic and aperture impedance (Coulter and Elzone) techniques. *Deep Res. II* 42, 139–157. doi: 10.1016/0967-0645(95)00009-f

Kiørboe, T. (2000). Colonization of marine snow aggregates by invertebrate zooplankton: abundance, scaling, and possible role. *Limnol. Oceanogr.* 45, 479–484. doi: 10.4319/lo.2000.45.2.0479

Kiørboe, T., Moehlenberg, F., and Hamburger, K. (1985). Bioenergetics of the planktonic copepod *Acartia tonsa*: relation between feeding, egg production and respiration, and composition of specific dynamic action. *Mar. Ecol. Prog. Ser. Oldend.* 26, 85–97. doi: 10.3354/meps026085

Kiørboe, T., and Thygesen, U. H. (2001). Fluid motion and solute distribution around sinking aggregates. II. Implications for remote detection by colonizing zooplankters. *Mar. Ecol. Prog. Ser.* 211, 15–25. doi: 10.3354/meps211015

Koski, M., Boutorh, J., and De La Rocha, C. (2017). Feeding on dispersed vs. aggregated particles: the effect of zooplankton feeding behavior on vertical flux. *PLoS One* 12:e0177958. doi: 10.1371/journal.pone.0177958

Koski, M., Breteler, W. K., and Schogt, N. (1998). Effect of food quality on rate of growth and development of the pelagic copepod *Pseudocalanus elongatus* (Copepoda, Calanoida). *Mar. Ecol. Prog. Ser.* 170, 169–187. doi: 10.3354/meps170169

Koski, M., Kiørboe, T., and Takahashi, K. (2005). Benthic life in the pelagic: aggregate encounter and degradation rates by pelagic harpacticoid copepods. *Limnol. Oceanogr.* 50, 1254–1263. doi: 10.4319/lo.2005.50.4.1254

Koski, M., Moller, E. F., Maar, M., and Visser, A. (2007). The fate of discarded appendicularian houses: degradation by the copepod, Microsetella norvegica, and other agents. *J. Plankton Res.* 29, 641–654. doi: 10.1093/plankt/fbm046

Lampitt, R. S., Noji, T., and Bodungen, B. V. (1990). What happens to zooplankton fecal pellets? Implications for material flux. *Mar. Biol.* 104, 15–23. doi: 10.1007/bf01313152

Lampitt, R. S., Wishner, K. F., Turley, C. M., and Angel, M. V. (1993). Marine snow studies in the Northeast Atlantic ocean: distribution, composition and role as a food source for migrating plankton. *Mar. Biol.* 116, 689–702. doi: 10.1007/bf00355486

Lenz, J., Morales, A., and Gunkel, J. (1993). Mesozooplankton standing stock during the North Atlantic spring bloom study in 1989 and its potential grazing pressure on phytoplankton: a comparison between low, medium and high latitudes. *Deep. Res. Part II* 40, 559–572. doi: 10.1016/0967-0645(93)90032-I

Li, W. K. W., McLaughlin, F. A., Lovejoy, C., and Carmack, E. C. (2009). Smallest algae thrive as the arctic ocean freshens. *Science* 326:539. doi: 10.1126/science.1179798

Lombard, F., Koski, M., and Kiørboe, T. (2013). Copepods use chemical trails to find sinking marine snow aggregates. *Limnol. Ocean.* 58, 185–192. doi: 10.4319/lo.2013.58.1.0185

Markussen, T. N., Konrad, C., Waldmann, C., Becker, M., Fischer, G., and Iversen, M. H. (2020). Tracks in the snow – advantage of combining optical methods to characterize marine particles and aggregates. *Front. Mar. Sci.* 7:476. doi: 10.3389/fmars.2020.00476

Marsay, C. M., Sanders, R. J., Henson, S. A., Pabortsava, K., Achterberg, E. P., and Lampitt, R. S. (2015). Attenuation of sinking particulate organic carbon flux through the mesopelagic ocean. *Proc. Natl. Acad. Sci. U.S.A.* 112, 1089–1094. doi: 10.1073/pnas.1415311112

Martin, J. H., Knauer, G. A., Broenkow, W. W., Bruland, K. W., Karl, D. M., Small, L. F., et al. (1983). Vertical transport and exchange of materials in the upper waters of the ocean (VERTEX): introduction to the program, hydrographic conditions and major component fluxes during VERTEX I. *Moss Land. Mar. Lab. Tech. Publ.* 83, 1–40. doi: 10.1007/978-1-4612-0353-7_1

Martin, J. H., Knauer, G. A., Karl, D. M., and Broenkow, W. W. (1987). VERTEX: carbon cycling in the northeast Pacific. *Deep Res.* 34, 267–285. doi: 10.1016/0198-0149(87)90086-0

Mayor, D. J., Anderson, T. R., Irigoien, X., and Harris, R. (2006). Feeding and reproduction of Calanus finmarchicus during non-bloom conditions in the Irminger Sea. *J. Plankton Res.* 28, 1167–1179. doi: 10.1093/plankt/fbl047

Mayor, D. J., Sanders, R., Giering, S. L. C., and Anderson, T. R. (2014). Microbial gardening in the ocean's twilight zone: detritivorous metazoans benefit from fragmenting, rather than ingesting, sinking detritus: fragmentation of refractory detritus by zooplankton beneath the euphotic zone stimulates the harvestable production of labile and nutritious microbial biomass. *Bioessays* 36, 1132–1137. doi: 10.1002/bies.201400100

Möller, K. O., John, M. S., Temming, A., Floeter, J., Sell, A. F., and Herrmann, J. P. (2012). Marine snow, zooplankton and thin layers: indications of a trophic link from small-scale sampling with the video plankton recorder. *Mar. Ecol. Prog. Ser.* 468, 57–69. doi: 10.3354/meps09984

Morata, N., and Seuthe, L. (2014). Importance of bacteria and protozooplankton for faecal pellet degradation. *Oceanologia* 56, 565–581. doi: 10.5697/oc.56-3.565

Ohtsuka, S., Kubo, N., Okada, M., and Gushima, K. (1993). Attachment and feeding of pelagic copepods on larvacean houses. *J. Oceanogr.* 49, 115–120. doi: 10.1007/BF02234012

Ploug, H., and Grossart, H. P. (2000). Bacterial growth and grazing on diatom aggregates: respiratory carbon turnover as a function of aggregate size and sinking velocity. *Limnol. Oceanogr.* 45, 1467–1475. doi: 10.4319/lo.2000.45.7.1467

Ploug, H., Iversen, M. H., and Fischer, G. (2008a). Ballast, sinking velocity, and apparent diffusivity within marine snow and zooplankton fecal pellets: implications for substrate turnover by attached bacteria. *Limnol. Oceanogr.* 53, 1878–1886. doi: 10.4319/lo.2008.53.5.1878

Ploug, H., Iversen, M. H., Koski, M., and Buitenhuis, E. T. (2008b). Production, oxygen respiration rates, and sinking velocity of copepod fecal pellets: direct measurements of ballasting by opal and calcite. *Limnol. Oceanogr.* 53, 469–476. doi: 10.4319/lo.2008.53.2.0469

Poulsen, L. K., and Iversen, M. H. (2008). Degradation of copepod fecal pellets: key role of protozooplankton. *Mar. Ecol. Prog. Ser.* 367, 1–13. doi: 10.3354/meps07611

Poulsen, L. K., and Kiørboe, T. (2005). Coprophagy and coprorhexy in the copepods Acartia tonas and *Temora longicornis*: clearance rates and feeding behaviour. *Mar. Ecol. Prog. Ser.* 299, 217–227. doi: 10.3354/meps299217

Poulsen, L. K., Moldrup, M., Berge, T., and Hansen, P. J. (2011). Feeding on copepod fecal pellets: a new trophic role of dinoflagellates as detritivores. *Mar. Ecol. Prog. Ser.* 441, 65–78. doi: 10.3354/meps09357

Reigstad, M., Riser, C. W., and Svensen, C. (2005). Fate of copepod faecal pellets and the role of *Oithona* spp. *Mar. Ecol. Ser.* 304, 265–270. doi: 10.3354/meps304265

Richter, C. (1994). *Regional and Seasonal Variability in the Vertical Distribution of Mesozooplankton in the Greenland Sea*. San Diego, CA: The University of California.

Ruiz, J. (1997). What generates daily cycles of marine snow? *Deep Res. Part I Oceanog. Res. Pap.* 44, 1105–1126. doi: 10.1016/s0967-0637(97)00012-5

Seuthe, L., Darnis, G., Riser, C. W., Wassmann, P., and Fortier, L. (2007). Winter–spring feeding and metabolism of Arctic copepods: insights from faecal pellet production and respiration measurements in the southeastern Beaufort Sea. *Polar Biol.* 30, 427–436. doi: 10.1007/s00300-006-0199-1

Shanks, A. L., and Edmondson, E. W. (1989). Laboratory-made artificial marine snow: a biological model of the real thing. *Mar. Biol.* 101, 463–470. doi: 10.1007/bf00541648

Siegenthaler, U., and Sarmiento, J. L. (1993). Atmospheric carbon dioxide and the ocean. *Nature* 365, 119–125.

Steinberg, D. K., Van Mooy, B. A. S., Buesseler, K. O., Boyd, P. W., Kobari, T., and Karl, D. M. (2008). Bacterial vs. zooplankton control of sinking particle flux in the ocean's twilight zone. *Limnol. Oceanogr.* 53, 1327–1338. doi: 10.4319/lo.2008.53.4.1327

Stemmann, L., Jackson, G. A., and Gorsky, G. (2004). A vertical model of particle size distributions and fluxes in the midwater column that includes biological and physical processes; Part II, application to a three year survey in the NW Mediterranean Sea. *Deep Res. I* 51, 885–908. doi: 10.1016/j.dsr.2004.03.002

Stemmann, L., Picheral, M., and Gorsky, G. (2000). Diel variation in the vertical distribution of particulate matter (>0.*15* mm) in the NW Mediterranean Sea investigated with the underwater video profiler. *Deep Sea Res. Part I Oceanogr. Res. Pap.* 47, 505–531. doi: 10.1016/S0967-0637(99)00100-4

Sun, J., and Liu, D. (2003). Geometric models for calculating cell biovolume and surface area for phytoplankton. *J. Plankton Res.* 25, 1331–1346. doi: 10.1093/plankt/fbg096

Svensen, C., Wexel Riser, C., Reigstad, M., and Seuthe, L. (2012). Degradation of copepod faecal pellets in the upper layer: role of microbial community and *Calanus finmarchicus*. *Mar. Ecol. Prog. Ser.* 462, 39–49. doi: 10.3354/meps09808

Swalethorp, R., Kjellerup, S., Dünweber, M., Nielsen, T. G., Møller, E. F., Rysgaard, S., et al. (2011). Grazing, egg production, and biochemical evidence of differences in the life strategies of *Calanus finmarchicus*, *C. glacialis* and *C. hyperboreus* in Disko Bay, Western Greenland. *Mar. Ecol. Prog. Ser.* 429, 125–144. doi: 10.3354/meps09065

Tamburini, C., Boutrif, M., Garel, M., Colwell, R. R., and Deming, J. W. (2013). Prokaryotic responses to hydrostatic pressure in the ocean - a review. *Environ. Microbiol.* 15, 1262–1274. doi: 10.1111/1462-2920.12084

Thiele, S., Fuchs, B. M., Amann, R., and Iversen, M. H. (2015). Colonization in the photic zone and subsequent changes during sinking determine bacterial community composition in marine snow. *Appl. Environ. Microbiol.* 81, 1463–1471. doi: 10.1128/aem.02570-14

van der Jagt, H., Friese, C., Stuut, J.-B. W., Fischer, G., and Iversen, M. H. (2018). The ballasting effect of Saharan dust deposition on aggregate dynamics and carbon export: aggregation, settling, and scavenging potential of marine snow. *Limnol. Oceanogr.* 63, 1386–1394. doi: 10.1002/lno.10779

Visser, A. W. (2001). Hydromechanical signals in the plankton. *Mar. Ecol. Prog. Ser.* 222, 1–24. doi: 10.3354/meps222001

Wassmann, P., Olli, K., Wexel Riser, C., and Svensen, C. (2003). "Ecosystem function, biodiversity and vertical flux regulation in the twillight zone," in *Marine Science Frontiers for Europe*, eds G. Wefer, F. Lamy, and F. Mantoura (Berlin: Springer-Verlag), 279–287. doi: 10.1007/978-3-642-55862-7_19

Weber, T., Cram, J. A., Leung, S. W., DeVries, T., and Deutsch, C. (2016). Deep ocean nutrients imply large latitudinal variation in particle transfer efficiency. *Proc. Natl. Acad. Sci. U.S.A.* 113, 8606–8611. doi: 10.1073/pnas.1604414113

Wiedmann, I., Reigstad, M., Sundfjord, A., and Basedow, S. (2014). Potential drivers of sinking particle's size spectra and vertical flux of particulate organic carbon (POC): turbulence, phytoplankton, and zooplankton. *J. Geophys. Res. Ocean.* 119, 6900–6917. doi: 10.1002/2013JC009754

Conflict of Interest: The authors declare that the research was conducted in the absence of any commercial or financial relationships that could be construed as a potential conflict of interest.

The reviewer JT declared a past co-authorship with one of the authors MI to the handling editor.